H. Tavoosi
Department of Mechanical Engineering,
Isfahan University of Technology,
Isfahan 84156-83111, Iran

S. Ziaei-Rad
Department of Mechanical Engineering,
Isfahan University of Technology,
Isfahan 84156-83111, Iran

F. Karimzadeh
Department of Material Engineering,
Isfahan University of Technology,
Isfahan 84156-83111, Iran

S. Akbarzadeh[1]
Department of Mechanical Engineering,
Isfahan University of Technology,
Isfahan 84156-83111, Iran
e-mail: s.akbarzadeh@cc.iut.ac.ir

Experimental and Finite Element Simulation of Wear in Nanostructured NiAl Coating

In this paper, the wear of nanostructured NiAl coating was studied both experimentally and numerically. First, the nanocrystalline NiAl intermetallic powder was synthesized by mechanical alloying (MA) of aluminum and Ni powders. The coatings were deposited onto the low carbon steel substrate using high velocity oxy-fuel (HVOF) technique. Nanoindentation test was conducted to find out the mechanical properties of the coating. The dry wear tests were then performed using a pin-on-block test rig under different operating conditions. Finally, finite element (FE) method was employed to model the wear characteristics of the prepared nanostructured material. A three-dimensional (3D) FE model was created and used to simulate the pin-on-block experiments. The results show that the volume losses predicted by the numerical analysis are in good agreement with the experimental data. [DOI: 10.1115/1.4030683]

Keywords: wear testing, nanoindentation, nanotribology, finite element modeling, wear modeling

1 Introduction

Wear is one of the destructive mechanisms that can deteriorate performance of many mechanical components such as gears in automobiles, airplanes, and pumps. It causes the reduction of component life and reliability. The high surface to volume ration along with the importance of grain size, grain boundary, dislocation density, and porosity has made the study of nanostructured materials an attractive subject.

NiAl intermetallic, because of its excellent oxidation resistance, high thermal conductivity, low density, and high melting point, is a suitable material for coating different industrial components to improve their wearing, corrosion, and oxidation resistance [1]. It can be used in different mechanical components such as gas turbine engine, rotor blades, and stator vanes. These coatings are brittle especially at ambient temperature [2]. One of the possible methods to overcome this problem is nanocrystallization of NiAl, which can improve the material ductility [3].

MA is one of the methods of production of nanocrystalline materials [4,5]. Two methods were found for NiAl formation during MA: (1) a rapid exothermic reaction and (2) a gradual diffusional process [6–10]. The powder prepared by MA can be deposited on surfaces using different thermal spraying techniques including HVOF process. The coatings prepared by this method have low porosity and high hardness and are relatively well stuck to the substrate [1]. HVOF technique produces denser coatings with excellent mechanical properties in comparison to other thermal spraying methods [2]. Recently, Hearley et al. [11,12] prepared NiAl intermetallic coatings by HVOF thermal spraying and investigated the effect of spray parameters on their properties and erosion behavior. Hu et al. [13] prepared nanostructured NiAl intermetallic coating by HVOF processing. Enayati et al. [14,15] prepared nanostructured NiAl coatings by MA and HVOF techniques and studied the microstructural and mechanical properties of coatings.

Pin-on-disk/block tribometry is the most commonly used experimental technique to study the tribological performance of a material pair of interest due to its simplicity and cost effectiveness. Since the tribosystem parameters, such as contact conditions, can be strongly different in practice, these tribotests are not adequate for accurate wear prediction in the design phase. Another method to incorporate wear into design is to perform full-scale tribotests that may mimic operating conditions. This technique, however, is time consuming and can be very expensive. Therefore, to evaluate and compare different designs with respect to wear, a simulation strategy in association with the FE method can fill the gap between in situ wear measurements on the one hand and tribometry on the other hand.

Recently, many efforts have been put into developing wear analysis and simulation techniques. In most of recent simulations, the contact geometry varies gradually and results of each step put into an iterative procedure in which the contact pressure and sliding distances are altered.

Rezai et al. [16] used an adaptive wear modeling method in ABAQUS to study the wear progress in radial sliding bearings contacting with a rotary shaft. The effect of bearing radial clearance on the wear depth was studied, and the results showed that while the wear depth is directly dependent on clearance size, the wear volume is not influenced considerably by the initial clearance size.

Hegadekatte et al. [17,18] developed a wear model known as global incremental wear model. In this method, the material removal is performed incrementally based on the contact pressure and mechanical and geometrical properties using the famous Archard's wear equation. They simulated the wear depth in ring-on-ring as well as pin-on-disk test using adaptive FE modeling.

Soderberg and Andersson [19] used the commercial FE package ANSYS to predict the wear in a composite pad–rotor interface. Their model was also based on the Archard's wear equation. They assumed that the rotor is a rigid body and then further simplified the analysis by assuming a linear isotropic material model.

Martinez et al. [20] simulated the sliding wear of polymer–metal contact pair by 3D model geometries in ABAQUS. This material pair corresponds to a specific contact in a mechanical element between a guide shoe insert and the corresponding guide. In this method, a subroutine named UMESHMOTION and adaptive meshing technique are jointly used to perform material removal. They conducted some wear experiments using the reciprocating flat-on-flat tribometer to validate their results.

[1]Corresponding author.
Contributed by the Tribology Division of ASME for publication in the JOURNAL OF TRIBOLOGY. Manuscript received January 7, 2015; final manuscript received May 12, 2015; published online July 1, 2015. Assoc. Editor: Dae-Eun Kim.

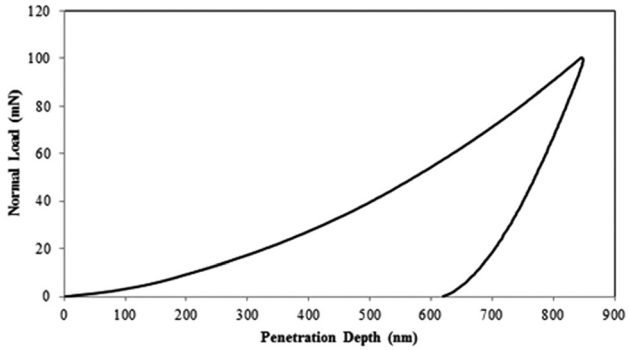

Fig. 1 The force displacement diagram of nanoindentation test

Table 1 Specifications of nanostructured NiAl measured from nanoindentation test

Elastic modulus (GPa)	Poisson's ratio	Hardness (GPa)
175±10	0.32	7.8±0.05

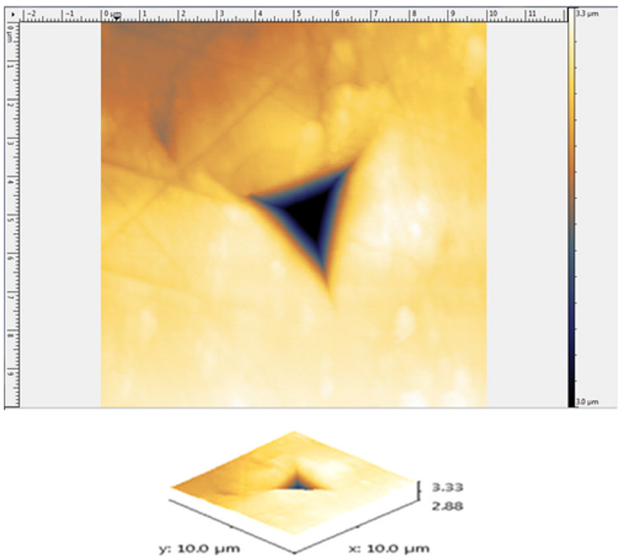

Fig. 2 Atomic force microscopy (AFM) images of nanostructured NiAl surface after indentation

Bortoleto et al. [21] investigated the wearing and frictional behavior of metals. They conducted dry pin-on-disk wear tests and then successfully simulated the contact by using the commercial FE software ABAQUS. They assumed that both pin and disk are deformable and have an elastic–plastic behavior. The comparison of simulation and experimental data shows that this method predicts reasonable wear behavior in the mild wear regime.

In this paper, the wear of nanostructured NiAl coating is experimentally and numerically studied. First, nanocrystalline NiAl intermetallic powder was synthesized by MA and deposited on a low carbon steel substrate by HVOF technique. Then, nanoindentation test was carried out using a diamond Berkovich indenter, and the results were used to find the mechanical and surface properties of the prepared nanostructured NiAl such as hardness, Young's module, and Poisson's ratio. In addition, pin-on-block tests were conducted on nanostructured NiAl samples in order to find out friction and wear behavior. Finally, a 3D deformable model of pin-on-block tribometer is simulated, and the local

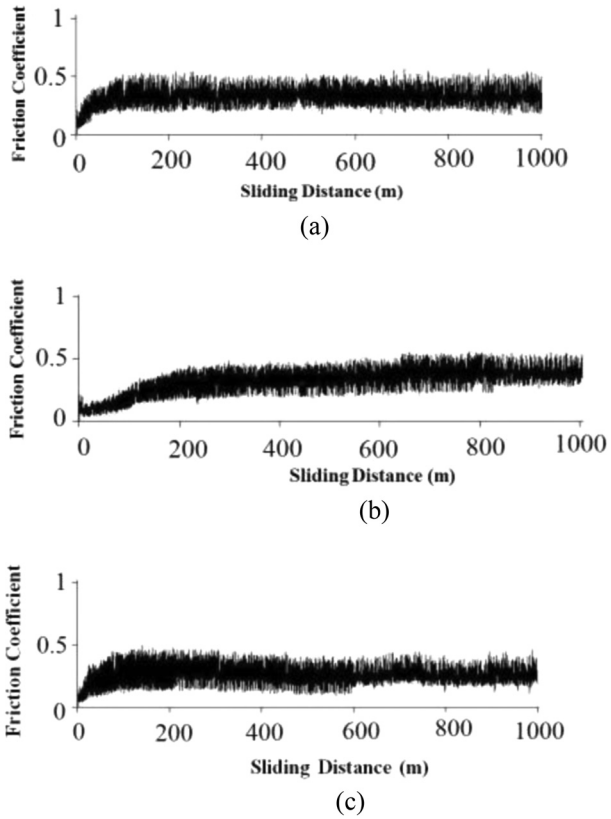

Fig. 3 Friction coefficient profiles for nanostructured NiAl coating: (*a*) 30 N, (*b*) 60 N, and (*c*) 90 N

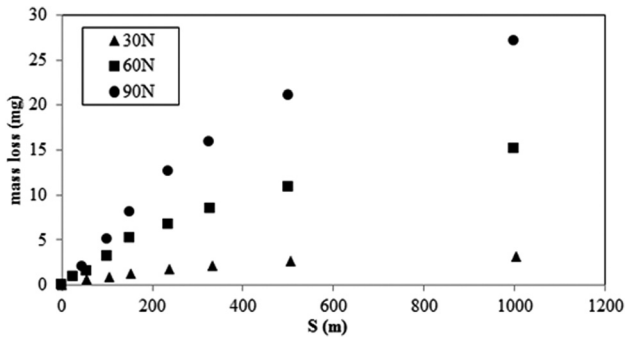

Fig. 4 Mass loss of coating during dry sliding wear tests for three different loads (maximum standard deviation is about 1 mg)

wear evolution is modeled using the Archard's equation. A wear-processing program has been developed using FORTRAN, which can calculate and implement the incremental wear evolution into the FE model.

2 Materials and Experiments

2.1 MA and HVOF Processing. Nanocrystalline NiAl intermetallic powder was prepared by MA of aluminum (particle size of 50–70 μm) and Ni (particle size of 30–110 μm) powders. The coatings were deposited onto the low carbon steel substrate by HVOF with a set of spraying parameters. The details of nanostructured NiAl coating procedure are discussed in the literature [14,15]. The crystallite size of NiAl phase was obtained from transmission electron microscopy observations. The results

Table 2 Wear test results of nanostructured NiAl after 1000 m of sliding under different loads

Parameters	30 N	60 N	90 N
Wear-rate (mg/m)	3	15	27
Wear coefficient (1/TPa)	0.014027	0.035068	0.0421

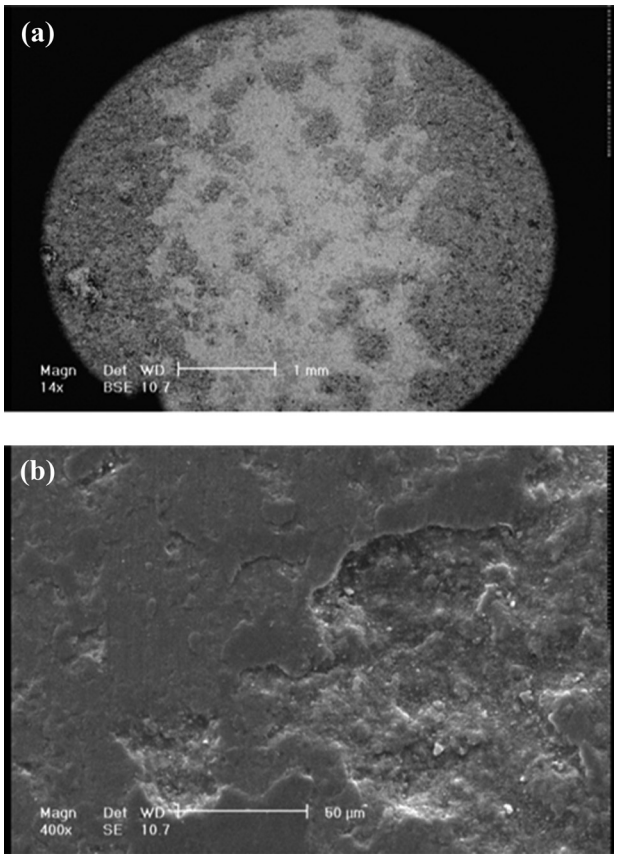

Fig. 5 Scanning electron microscope (SEM) of the specimen surface with (*a*) 14× magnification and (*b*) 400× magnification

showed that after HVOF thermal spray process, the obtained NiAl grain size in the coating was about 20 nm.

2.2 Nanoindentation Test. A commercial nanoindenter-R IIs (Nano Instruments, Inc.) equipped with a diamond Berkovich indenter was used to perform the nanoindentation experiments. The machine applies a force on the test specimen, which gradually rises from zero to the maximum load of 100 mN and then the load is removed. The loading and unloading rate for the force was 200 mN/min. The data acquisition rate was 10 Hz.

Experiments were repeated six times at different positions on a sample surface to ensure statistical reliability, and the averaged results were chosen as the final data. The hardness and elastic modulus of the nanostructured NiAl can be estimated from the measured curves shown in Fig. 1 using the method described by Oliver and Pharr [22]. Table 1 shows the measured values for these parameters. The value of the Poisson's ratio has been obtained from Ref. [23]. Two different images of AFM from the nanostructured NiAl surface after indentation are shown in Fig. 2.

2.3 Pin-on-Block Test. The wear tests were performed with a pin-on-block test rig without lubrication. The block movement was reciprocating with a sliding speed of 0.08 m/s. The pin is made of AISI 52,100 with 5 mm diameter, 50 mm height, and 5 mm curvature radius of the tip of the pin, and the block has 100 mm length, 30 mm width, and 5 mm thickness of which 0.2 mm of total thickness was the nanostructured NiAl coating and the remaining 4.8 mm thickness corresponds to the carbon steel substrate.

The normal load applied on the pin was 30, 60, and 90 N. The contact pressures corresponding to each of these applied loads are 1.1 GPa, 1.4 GPa, and 1.6 GPa, respectively. The tests were stopped after a sliding distance of 1000 m. The variation of mass at sliding distances of 25, 50, 100, 150, 200, 500, and 1000 m was measured using a scale with precision of 0.1 mg. Figure 3 compares the mass loss values of coating during dry sliding wear test under three loads of 30, 60, and 90 N, respectively. According to Fig. 4, the wear-rate of all three loads is initially high, but the wear-rate gradually reduces. At early stages of the wear test, the real area of contact is small, and thus, the contact pressure is high. Gradually, as the material is removed, the real area of contact increases, and therefore, the contact pressure decreases, resulting in a decrease in the wear coefficient. Table 2 shows the calculated wear coefficients for nanostructured NiAl coating in wear test.

The friction force was continuously measured during the wear test via a programmable logic controller. The values of friction coefficient were determined by the ratio between the friction force and the applied normal force. Figure 3 shows the variation of friction coefficient versus sliding distance for coating under three loads. The friction coefficient initially increases and then reaches a steady-state value due to wear of asperities and formation of wear debris. The average friction coefficient of coating was found to be around 0.4.

Careful surface observations using SEM indicate that initially abrasive wear is the dominant wear regime. During running-in, an oxide layer is formed, which results in the adhesive wear to become the dominant wear regime. Figure 5(*a*) shows the surface

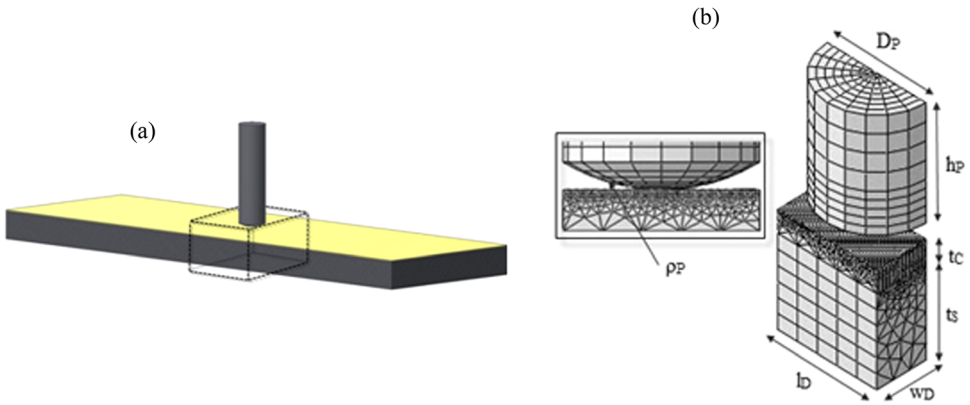

Fig. 6 (*a*) Whole scale test setup of pin-on-block in dry sliding and (*b*) FE model

Table 3 Geometrical parameters of FE model

Parameter	Value (mm)
Pin diameter (D_P)	5
Pin height (h_P)	5
Pin curvature radius (ρ_P)	5
Block length (l_D)	5
Block wide (w_D)	5
Substrate thickness (t_S)	4.8
Coating thickness (t_C)	0.2

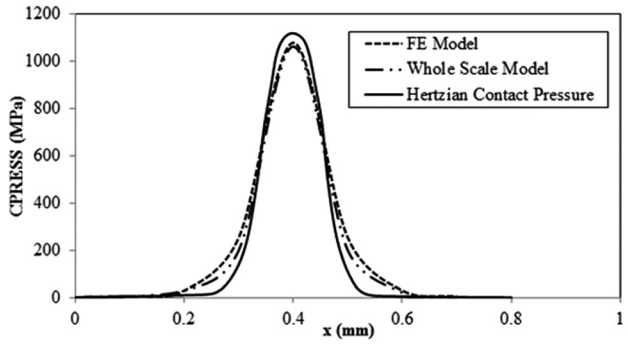

Fig. 7 Contact pressure profiles of whole scale and FE model in comparison with Hertz solution at 30 N load

of the specimen with a magnification of 14×. The same surface has been illustrated with 400× magnification in Fig. 5(*b*).

3 Numerical Model

Wear simulation in a general tribosystem is carried out by two steps: the first step is the solution of the contact problem equilibrium equation and the second step is using this solution to predict the wear.

The prediction of wear was implemented according to Archard's formula, in which the worn volume V (m^3) or the wear depth h (m) are defined as follows:

$$\frac{V}{S \cdot A} = \frac{h}{S} = \frac{k}{H} P \tag{1}$$

where S (m) is the sliding distance, A (m^2) is the apparent contact area, P (Pa) is the normal contact pressure, and H (Pa) is the hardness of the softer material. The dimensionless constant k is the wear coefficient that characterizes the wear resistance of the contact, and the ratio k/H ($m^2\ N^{-1}$) is known as the specific wear-rate.

The Archard's formula can alternatively be expressed as

$$\frac{dh}{ds} = \frac{k}{H} P \tag{2}$$

The pin and disk geometry as well as the loading and materials' specifications are the inputs to this model. Then, using the FE software, the pressure at each node is calculated. Using the wear coefficient and material's hardness and employing a specific subroutine, the wear depth at each node is calculated and the locations of the nodes are updated. The adaptive meshing technique is used to impose the wear on the surface and relocate the internal nodes. The new geometry is then used as the input to this algorithm.

The geometrical details of the pin-on-block tribometer test setup are shown in Fig. 6(*a*). Only the geometry inside the dashed cube is used for the FE simulation. The FE model is shown in Fig. 6(*b*). The values of the parameters shown in Fig. 6(*b*) are listed in Table 3. The results from the contact simulation depend on the mesh size. Therefore, a more refined mesh was generated near the contact region, and a coarser mesh was used in locations away from the contact region. The chosen element type for pin and coating is an eight-node linear brick element, and the element type of the substrate is a six-node linear triangular prism element.

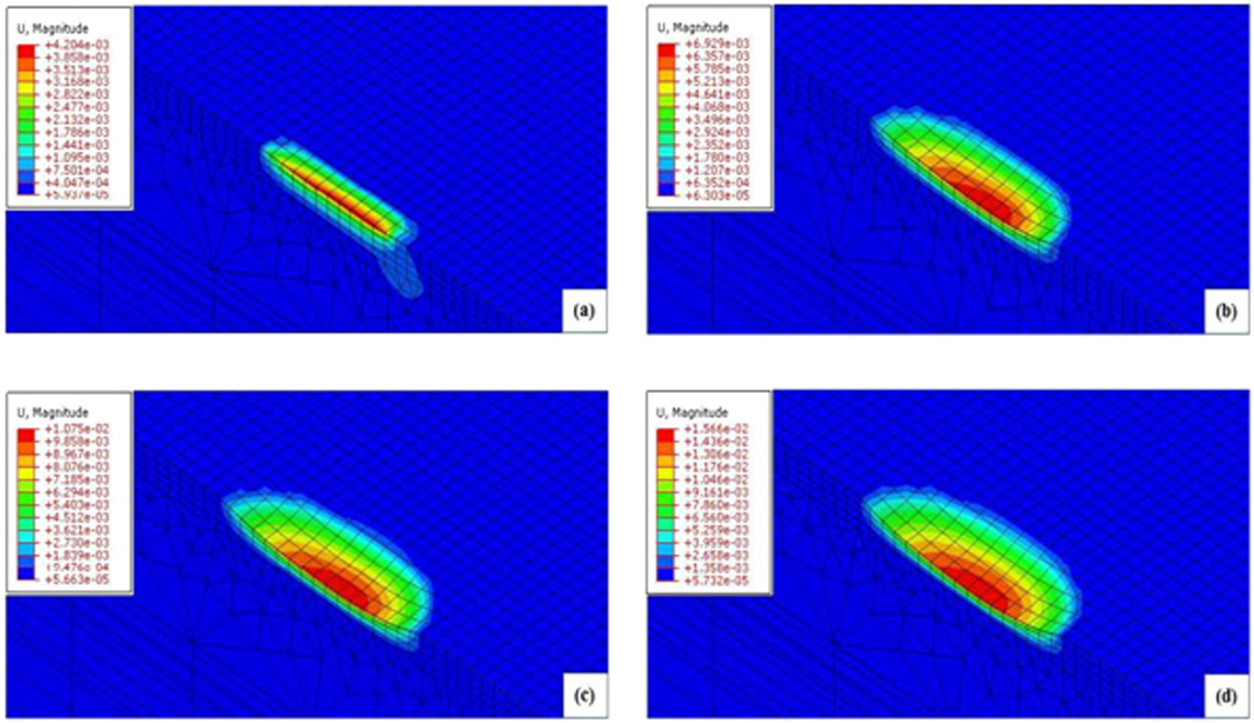

Fig. 8 Superposition of elastic deformation effect and wear on block surface under 30 N load at: (*a*) after 800 wear cycle, (*b*) after 2600 wear cycle, (*c*) after 6300 wear cycle, and (*d*) after 12500 wear cycle

The materials used for pin was steel with Young's modulus of $E = 210$ GPa and Poisson's ratio $\nu = 0.3$. The block mechanical properties are described in Table 1.

The following boundary conditions and loads were applied to the FE models, which are based on the following experimental conditions:

- Three different load conditions, with normal loads of 30, 60, and 90 N, are applied on the top of the pin.
- Displacements and rotations of block were constrained in all directions.
- In order to provide the reciprocating motion of the pin along the length of the block at each wear cycle, a displacement was imposed to the pin along the length of the block.
- Since both of geometries and loads of the model were symmetric about the width of the block, symmetrical conditions were considered relative to axis along the width of the block.
- The friction coefficient was considered as an input parameter to the model.

In order to make sure that the FE model predicts an appropriate pressure profile, the contact pressure profile for the whole model and the solution of contact stresses for a Hertzian circular contact area corresponding to the load of 30 N were calculated and compared to the FE prediction in Fig. 7. The results indicate that the FE model estimates the pressure distribution between the pin and the block with a good accuracy, and therefore, the model can be safely used for the wear calculation.

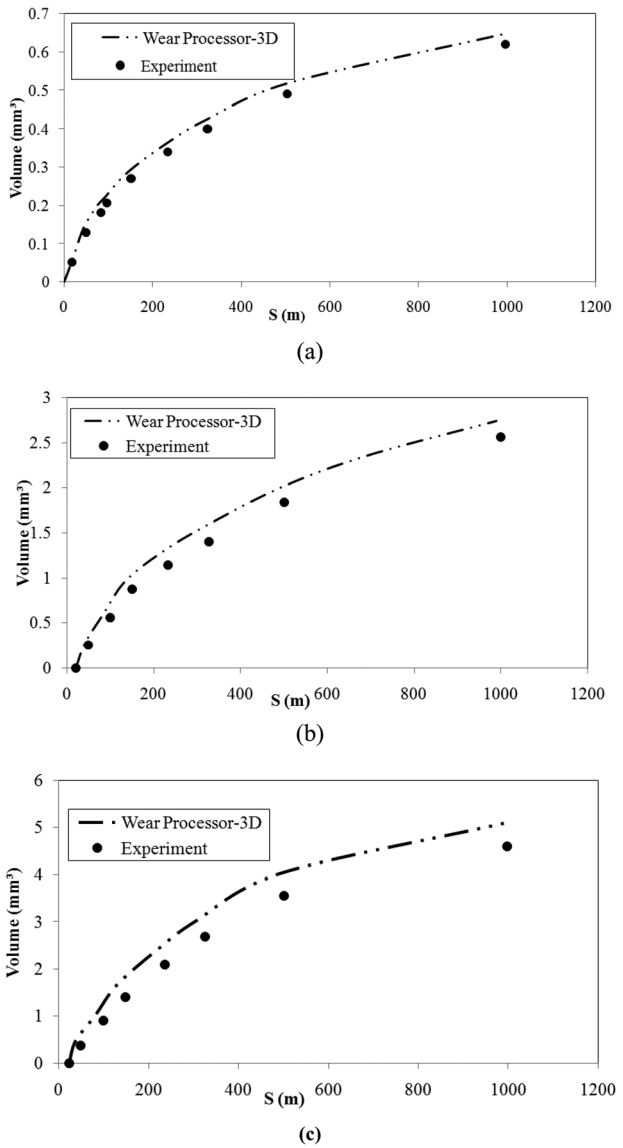

Fig. 9 Comparison between block volume losses of experimental and numerical results along the 1000 m sliding under (*a*) 30 N, (*b*) 60 N, and (*c*) 90 N load (maximum standard deviation in experiment data is about 0.6 mm^3)

4 Results and Discussion

The result from the wear simulation is presented in Fig. 8, which shows the displacement of nodes at the block surface in the direction perpendicular to the contact area at different stages of sliding under 30 N load. It can be observed from Figs. 8(*a*)–8(*d*) that during the sliding, the contact area increases as a result of wear. Therefore, the contact pressure and subsequently the wear rate decrease.

Figure 9 presents a comparison between experimental and numerical block volume losses due to sliding wear under three loads of 30, 60, and 90 N. Predicted values were obtained from numerical extrapolation, in which the wear volume simulated during 1 mm displacement of the pin over the block surface was assumed to be constant throughout the entire test. The volume losses obtained with the numerical analysis seem to be greater than the experimental ones.

The reason is due to the fact that the dimensionless wear coefficient obtained from experimental results was overestimated because both running-in and steady-state periods were considered at experimental test. This results in a global wear coefficient and provides higher volume losses when steady-state conditions are involved, as assumed in the simulations. Therefore, one can observe that the difference between numerical and experimental results was lower for 30 N, due to its shorter running-in period, as shown in Fig. 4.

Another possible reason for the difference between experimental and predicted volume losses especially at final stages of experiment is due to thermal effects. In fact, due to the contact of asperities, the wear-rate is higher at initial stages of the experiment. As a result of friction effects, an oxide layer is formed on the block surface and it causes reduction of wear-rate. Since the thermal effects are ignored in the simulation, the predicted wear rate is larger than the experimentally measured values.

In addition, the adhesion phenomena during sliding can be observed at large normal loads. These phenomena can increase the block volume due to material transfer between surfaces; actually, debris from pin adhere at block surface. This is due to the fact that the numerical approach was not able to consider the gain of adhered volume in the block at high normal loads.

5 Conclusions

In this study, nanocrystalline NiAl intermetallic powder was synthesized by MA and then deposited on a low carbon steel substrate by HVOF technique. Nanoindentation test was performed on the synthesized coating to obtain its mechanical properties. The test results indicate that the coating has a modulus of elasticity of 174.72 GPa and a hardness value of 7860.8 MPa. To identify the wear characteristics of the nanostructured NiAl, pin-on-block experiments were conducted by applying 30, 60, and 90 N normal loads on pin and the tests were continued for a distance of 1000 m. The variation of mass at different sliding distances was determined. The test results indicate an initial high wear-rate, which gradually reduces. In fact, at early stages of the wear test, surface roughness reduces the actual area of surface contact between the coating layers and the steel pin.

Finally, a 3D FE model was created. The results indicate good agreement between block volume losses obtained from simulation and experimental data along a 1000 m sliding distance.

References

[1] Sidhu, T. S., Prakash, S., and Agarwal, R. D., 2006, "Performance of High-Velocity Oxy-Fuel Sprayed Coatings on an Fe-Based Superalloy in

Na_2SO_4–60%V_2O_5 Environment at 900 °C. Part I: Characterization of the Coatings," Mater. Eng. Perform., **15**(1), pp. 130–138.
[2] Herman, H., Sampath, S., and Mccune, R., 2000, "Thermal Spray: Current Status and Future Trends," MRS Bull., **25**(7), pp. 17–25.
[3] Liu, C. T., Stiegler, J. O., and Froes, F. H., 1990, *Ordered Intermetallics: ASM Metals Handbook*, 10th ed., ASM, Materials Park, OH.
[4] Koch, C. C., and Whittenberger, J. D., 1996, "Mechanical Milling/Alloying of Intermetallics," Intermetallics, **4**(5), pp. 339–355.
[5] Froes, F. H., Suryanarayana, C., Russel, K., and Li, G. C., 1995, "Synthesis of Intermetallics by Mechanical Alloying," Mater. Sci. Eng., A, **192–193**(Pt. 2), pp. 612–623.
[6] Joardar, J. S., Pabi, K., and Murty, B. S., 2007, "Milling Criteria for the Synthesis of Nanocrystalline NiAl by Mechanical Alloying," J. Alloys Compd., **429**(1–2), pp. 204–210.
[7] Chen, T., Hampikian, J. M., and Thadhani, N. N., 1999, "Synthesis and Characterization of Mechanically Alloyed and Shock-Consolidated Nanocrystalline NiAl Intermetallic," Acta Mater., **47**(8), pp. 2567–2579.
[8] Murty, B. S., Mohan Rao, M., and Ranganathan, S., 1995, "Milling Maps and Amorphization During Mechanical Alloying," Acta Metall. Mater., **43**(6), pp. 2443–2450.
[9] Enayati, M. H., Karimzadeh, F., and Anvari, S. Z., 2008, "Synthesis of Nanocrystalline NiAl by Mechanical Alloying," J. Mater. Process. Technol., **200**(1–3), pp. 312–315.
[10] Mashreghi, A., and Moshksar, M. M., 2009, "Partial Martensitic Transformation of Nanocrystalline NiAl Intermetallic During Mechanical Alloying," J. Alloys Compd., **482**(1–2), pp. 196–198.
[11] Hearley, J. A., Little, J. A., and Sturgeon, A. J., 2000, "The Effect of Spray Parameters on the Properties of High Velocity Oxy-Fuel NiAl Intermetallic Coatings," Surf. Coat. Technol., **123**(2–3), pp. 210–218.
[12] Hearley, J. A., Little, J. A., and Sturgeon, A. J., 1999, "The Erosion Behaviour of NiAl Intermetallic Coatings Produced by High Velocity Oxy-Fuel Thermal Spraying," Wear, **233–235**, pp. 328–333.
[13] Hu, W., Li, M., and Masahiro, F., 2008, "Preparation and Properties of HVOF NiAl Nanostructured Coatings," Mater. Sci. Eng., A, **478**(1–2), pp. 1–8.
[14] Enayati, M. H., Karimzadeh, F., and Tavoosi, M., 2011, "Nanocrystalline NiAl Coating Prepared by HVOF Thermal Spraying," J. Therm. Spray Technol., **20**(3), pp. 440–446.
[15] Enayati, M. H., Karimzadeh, F., and Jafari, M., 2014, "Microstructural and Wear Characteristics of HVOF-Sprayed Nanocrystalline NiAl Coating," Wear, **309**(1–2), pp. 192–199.
[16] Rezai, A., Paepagem, W. V., and Baets, P. D., 2012, "Adaptive Finite Element Simulation of Wear Evolution in Radial Sliding Bearings," Wear, **296**(1–2), pp. 660–671.
[17] Hegadekatte, V., Huber, N., and Kraft, O., 2006, "Modeling and Simulation of Wear in a Pin on Dics Tribometer," Tribol. Lett., **24**(1), pp. 51–60.
[18] Hegadekatte, V., Huber, N., and Kraft, O., 2004, "Finite Element Based Simulation of Dry Sliding Wear," Modelling Simul. Mater. Sci. Eng., **13**(1), pp. 57–75.
[19] Soderberg, A., and Andersson, S., 2009, "Simulation of Wear and Contact Pressure Distribution at the Pad-to-Rotor Interface in a Disc Brake Using General Purpose Finite Element Analysis Software," Wear, **267**(12), pp. 2243–2251.
[20] Martinez, F. J., Canales, M., Lzquierdo, S., Jimenez, M. A., and Martinez, M. A., 2012, "Finite Element Implementation and Validation of Wear Modeling in Sliding Polymer–Metal Contacts," Wear, **284–285**, pp. 52–64.
[21] Bortoleto, E. M., Rovani, A. C., Seriacopi, V., Zachariadis, D. C., and Machado, I. F., 2013, "Experimental and Numerical Analysis of Dry Contact in the Pin on Disc Test," Wear, **301**(1–2), pp. 19–26.
[22] Oliver, W. C., and Pharr, G. M., 1992, "An Improved Technique for Determining Hardness and Elastic Moduli Using Load and Displacement Sensing Indentation Experiments," Mater. Res., **7**(6), pp. 1564–1583.
[23] Toparli, M., Sen, F., Culha, O., and Celik, E., 2007, "Thermal Stress Analysis of HVOF Sprayed WC–Co/NiAl Multilayer Coatings on Stainless Steel Substrate Using Finite Element Methods," Mater. Process. Technol., **190**(1–3), pp. 26–32.